Determination of Temperature Rise in a Dry Type Transformer using Finite Element Analysis

G. H. Chitaliya* and S. K. Joshi**
*-**Dept. of Electrical Engineering, Faculty of Tech. & Engineering, The M. S. University of Baroda, Baroda, Gujarat, India
ghchitaliya@gmail.com, skjoshi@ieee.org

Abstract: This paper represents the effectiveness of finite element method in designing a dry type transformer to determine the temperature rise. A 160 kVA Vacuum Pressure Impregnated (VPI) tap wound LT isolation transformer having nominal voltage ratio of 415 / 415 Volt has been designed and subjected to a temperature rise test by simulation load method. A 3D finite element method using Variational Approach was adopted in designing the transformer to estimate the temperature rise under full load condition for linear loads.

Keywords: Transformer, Temperature rise, 3D Variational Approach, Finite Element Method (FEM).

Introduction

The finite element method is being used since long for different applications like to determine forces in a civil structure, to carry out stress analysis in a mechanical structure, to identify vibration and shocks effect on a structure or components, thermal analysis of an equipment or their part etc. The FEM has been utilized effectively for doing the analysis of various electrical equipments like inductors, generators, transformers, etc. A. G. Kladas, M. P. Papadopoulos and J. A. Tegopoulos [9], represent use of FEM for finding the leakage flux and force in a winding of a power transformer during short circuit condition. A. S. Reddy and M. Vijaykumar [3], have calculated the life of a power transformer by identifying the hottest spot in a winding using finite element method. M. Lee, H. A. Abdullah, J. C. Jofriet and D. Patel have adopted 2 Dimensional approach using Quasi-Static FEM and circuit based method [11, 12]. M. R. Barzegaram, M. Mirzaie and A. S. Akmal [2] did the analysis in a power transformer to detect the short circuits in winding because of inter-turn or disk to disk failures with the help of Frequency Response method. References [4], [5], [7] & [8] also discuss different methods to design transformer using Finite Element Method.

The short circuit study of a transformer having a split winding has been represented by G. B. Kumbhar and S. V. Kulkarni [6] with an approach of coupled field circuit. In the study the estimation of forces due to short circuit on a winding has been found by FEM. However, they did not estimate an actual deformation due to mechanical forces. H. M. Ahn, Y. H. Oh, J. K. Kim, J. S. Song and S. C. Hahn, [1] have taken care of mechanical forces on a dry type transformer of 50 KVA with due verification through experiments.

In present paper the main focus is on the determination of temperature rise in a dry type transformer. Finite Element Method has been used to determine the temperature rise in a 160 kVA, three phase, Dyn1, 415 V / 415 V, 50 Hz, dry type Vacuum Pressure Impregnated tap wound transformer, when being subjected to temperature rise by simulation load method in accordance to IS 11171 -1985 / IS 2026-2011 [20].

The hot spot in any electrical machine is due to losses in it. The hot spot temperature is to be determined for estimating the life of insulating material and consequently that of a machine. In a transformer the heat flow is through core and through winding and insulation. It mainly depends on its geometry and type of construction.

The temperature distribution in core and winding has been estimated using 3D Variational approach and overall temperature rise has been calculated. Based on FEM results, a design modification has been done for better air circulation and a transformer has been manufactured which then sent to Electrical Research & Development Association (ERDA), Vadodara, Gujarat, India for an actual thermal run (temperature rise test).

The transformer model has been shown in Fig. 1 and its specifications are as given in Table 1.

Thermal Capacity of a Dry Type Transformer

In a dry type transformer the construction is critical for maintaining the thermal capacity. Thermal capacity is defined by its ability to supply the rated load within predefined temperature rise limit in connection with the temperature rise limits of the insulating materials used.

The parameters governing the temperature rise are no load losses, load losses and the space between core and winding. The volume of core and winding plays a vital role in heat dissipation.

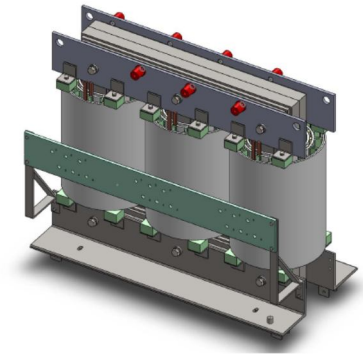

Fig 1. Transformer Model

Table 1. Specification of 160 kVA Transformer

Type of Transformer	**Dry type Double Wound**
Rating	160 kVA, 50 Hz, 3 Phase
Impregnation	Vacuum Pressure Impregnated
Insulation Class	H,
Input / Output Voltage	415 V (Delta) / 415 V (Star)
Impedance	4%
Duty / Vector Group	Continuous / Dyn1
Core/Copper Losses	1000 / 2400 at 75 ° C in W (Max)
Temperature Rise Limit	70 °C (Within Insulation Class B limit)
Reference Standard	IS 11171/2026

Heat Dissipation in Core

The transformer core consists of silicon steel laminations insulated from each other having thickness varying from 0.5 mm to 0.23 mm or even less. Due to alternate magnetization of the core, iron losses takes place which in turn produces heat.

Fig. 2 shows an elemental core of a transformer. The centre of the core is its hottest part. The heat dissipation will be through conduction at surfaces A (heat flow along X axis across the lamination) and B (heat flow along Z axis along the lamination) and through convection in direction C (Y axis).

The temperature of the hottest spot is described as [13, 16]

$$\theta_m = \frac{q\rho t^2}{8} + \theta_s \tag{1}$$

where, q is the heat produced per unit volume in W/m^3, t is the lamination thickness in m, ρ is the thermal resistivity of the material along the direction of heat flow in °C m/W and θ_s is the initial surface temperature of the core in °C.

The temperature gradient along A, B and C directions can be expressed as

$$\theta_a = \frac{q\rho_a t^2}{2}, \theta_b = \frac{q\rho_b t^2}{2}, \theta_c = \frac{q\rho_c t^2}{2} \tag{2}$$

where, ρ_a, ρ_b and ρ_c are the thermal resistivity of the lamination across the core, along the core and that of air respectively.

Though the thermal resistivity along the core is quite low, the heat dissipation along the core is not that effective as the height of the core is quite large as compared to the thickness. This becomes more critical especially when the coil/winding construction is concentric layer type.

Also the thermal resistivity of air is quite large which do not help significantly in heat dissipation. The effective heat dissipation is across the lamination and because of the air flow through the ventilating duct either on the periphery of the core or within the core placed axially as per design requirement.

Heat Dissipation in Winding and Insulation

The transformer windings are consisting of non-homogenous surfaces and hence heat dissipation is not uniform and does not take place along the parallel paths only. As the windings have insulation in addition to copper, the thermal resistivity of built up windings depends upon the relative thickness of insulation to copper. The heat flow in a winding normally takes place in two directions – radially and axially outwards.

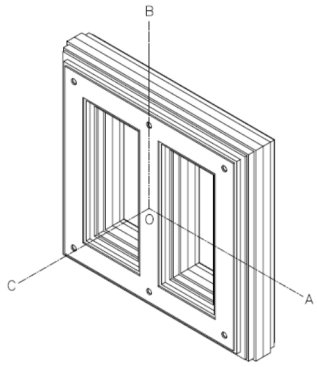

Fig 2. Elementary Core Model

The hot spot temperature in a transformer winding with square/rectangular geometry can be estimated by (3) and for cylindrical geometry by (4), [16].

$$\theta_{sr} = \frac{qlwt}{8l\left[\frac{w}{t\rho_x}+\frac{t}{w\rho_y}\right]} \tag{3}$$

where, l is the length (height) of the coil in m, t is the thickness of the coil in m, w is the width or outer diameter of the coil in m and ρ_x and ρ_y are thermal resistivity in radial and axial directions respectively in °C m/W

$$\theta_{cy} = \frac{q\rho_{co}t^2}{2} \tag{4}$$

where,
$\rho_{co} = \rho_i\left(1 - S_f{}^{0.5}\right)$ = thermal resistivity of coil in °C m/W
ρ_i = thermal resistivity of insulating material
S_f = Space factor = Copper area/total winding area

While determining the hot spot temperature of a winding, one must consider the effect of momentary overloads, the transformer is being subjected to, during its entire life span. For such overloads the temperature is calculated with assumption that all the heat developed is stored in the copper without dissipation. The temperature rise is then calculated using (5) [15].

$$\theta = at\left\{\frac{2T_1+at}{2T_1} + \frac{620K_d}{2T_1+at}\right\} \tag{5}$$

where,
t = overload duration in second
$T_1 = \theta_1 + 234.5$ °C
θ_1 = Initial temperature in °C
a = 0.0025*Total copper losses in W/kg at θ_1
K_d = Eddy current ratio at 75 °C
= Actual I^2R loss / DC I^2R loss
To estimate the hot spot temperature in the winding, due to combined effect of core losses and winding losses a FEM as shown in [1] is used. The flow chart for this is given in Fig. 3.

Heat Transfer Calculation using FEA
The heat conduction in an orthotropic solid body is governed by the differential equation [17] that is expressed as:

$$\frac{\partial}{\partial_x}\left(k_x\frac{\partial T}{\partial_x}\right) + \frac{\partial}{\partial_y}\left(k_y\frac{\partial T}{\partial_y}\right) + \frac{\partial}{\partial_z}\left(k_z\frac{\partial T}{\partial_z}\right) + q' = \rho c\frac{\partial T}{\partial t} \tag{6}$$

where, k_x, k_y, k_z are the thermal conductivities of the material in x, y and z direction respectively, T is the temperature, ρ is the density of the material, c is the specific heat of the material and q' is the rate of heat generated per unit volume.
Considering thermal conductivity in all the direction to be same, i.e. k_x, k_y, k_z=k, (6) reduces to

$$\frac{\partial^2 T}{\partial x^2} + \frac{\partial^2 T}{\partial y^2} + \frac{\partial^2 T}{\partial z^2} + \frac{q'}{k} = \frac{1}{\alpha}\frac{\partial T}{\partial t} \tag{7}$$

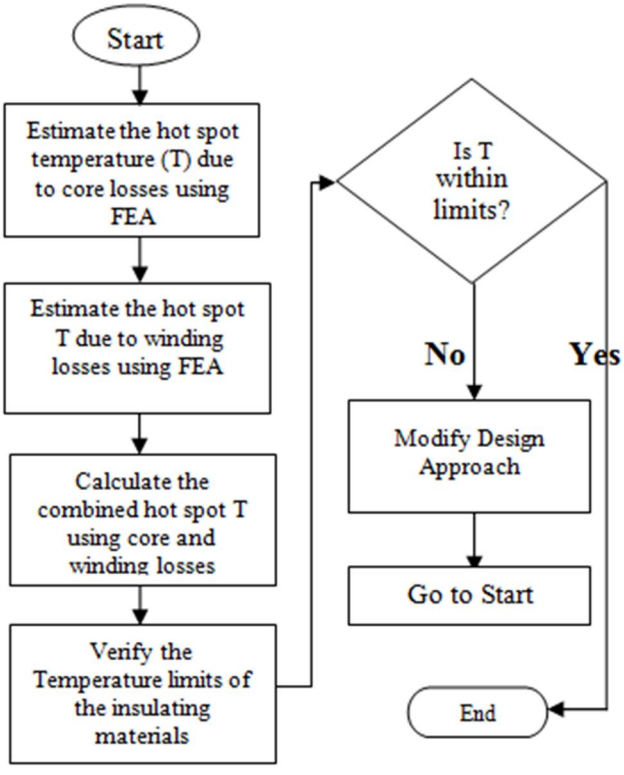

Fig 3. The Flow Chart for Thermal Analysis of Transformer

where
$\alpha = k/\rho c$ is known as thermal diffusivity.

Equation (7) is the equation for heat conduction which governs the distribution of temperature and the heat flow due to conduction in a solid with uniform material properties (isotropic body).

If body does not contain any heat source then (7) changes to the Fourier equation,

$$\frac{\partial^2 T}{\partial x^2} + \frac{\partial^2 T}{\partial y^2} + \frac{\partial^2 T}{\partial z^2} = \frac{1}{\alpha}\frac{\partial T}{\partial t} \tag{8}$$

When the body is having heat sources and is in a steady state, (7) become the Poisson's equation,

$$\frac{\partial^2 T}{\partial x^2} + \frac{\partial^2 T}{\partial y^2} + \frac{\partial^2 T}{\partial z^2} + \frac{q'}{k} = 0 \tag{9}$$

And when the body is without any heat source and is in a steady state, (7) becomes the Laplace equation

$$\frac{\partial^2 T}{\partial x^2} + \frac{\partial^2 T}{\partial y^2} + \frac{\partial^2 T}{\partial z^2} = 0 \tag{10}$$

Two boundary conditions required to be specified as the differential equations (7) or (8) - is of second order. The possible conditions are

$$T(x, y, z, t) = T_0 \text{ for } t > 0 \text{ on } S_1 \tag{11}$$

$$k_x \frac{\partial T}{\partial x} l_x + k_y \frac{\partial T}{\partial y} l_y + k_z \frac{\partial T}{\partial z} l_z + q_0 = 0 \text{ for } t > 0 \text{ on } S_2 \tag{12}$$

$$k_x \frac{\partial T}{\partial x} l_x + k_y \frac{\partial T}{\partial y} l_y + k_z \frac{\partial T}{\partial z} l_z + h(T - T_\infty) = 0 \text{ for } t > 0 \text{ on } S_3 \tag{13}$$

where q_0 is the heat flux at boundary, h is the heat transfer coefficient due to convection, T_∞ is the temperature of surroundings and l_x, l_y, l_z are the direction cosines of the outward drawn normal to the boundary.
The boundary condition (11) is applicable when the surface is self heating or in contact with melting solid or a boiling liquid, the second condition (12) is applicable when a thin film or patch heater is attached to the surface and the third condition (13) is applicable when cold or hot air flows around the surface.
Equation (7) or (8) is a first order equation in time t, and hence one initial condition is required, which is expressed as

$$T(x,y,z,t) = \bar{T}_0\,(x,y,z)\ in\ V \tag{14}$$

where V is the domain (volume) of the solid body and $\bar{T}_0$ is the specified temperature distribution at time zero.
In this paper, the finite element equations for the heat conduction problem have been derived using a Variational approach. The temperature distribution *T(x, y, z, t)* has been found inside the solid body by minimizing the integral function as shown in (15) that satisfies all boundary conditions and initial condition stated in (11) to (14).

$$I = \frac{1}{2}\iiint_V \left[k_x\left(\frac{\partial T}{\partial x}\right)^2 + k_y\left(\frac{\partial T}{\partial y}\right)^2 + k_z\left(\frac{\partial T}{\partial}\right)^2 - 2\left(\acute{q} - \rho c\frac{\partial T}{\partial t}\right)T\right]dV + \iint_{S_2} q_0 T dS_2 + \frac{1}{2}\iint_{S_3} h(T - T_\infty)^2 dS_3 \tag{15}$$

The step wise procedure involved in deriving the finite element equations is given below.
Step 1: Domain V is to be divided into E finite elements each having p nodes.
Step 2: Estimate the variation of T in each finite element with a suitable form and express it in element e as

$$T^{(e)}(x,y,z,t) = [N(x,y,z)]\vec{T}^{(e)} \tag{16}$$

where,

$$[N(x,y,z)] = \left[N_1(x,y,z)\quad N_2(x,y,z)\ \dots\ N_p(x,y,z)\right]$$

$$\vec{T}^{(e)} = \begin{Bmatrix} T_1(t) \\ T_2(t) \\ \cdot \\ \cdot \\ \cdot \\ T_p(t) \end{Bmatrix}^{(e)}$$

$T_i(t)$ is the temperature of node *i* and $N_i(x, y, z)$ is the interpolation function corresponding to node i of element e.
Step 3: The functional *I* is to be expressed as a sum of E elemental quantities $I^{(e)}$ as

$$I = \sum_{e=1}^{E} I^{(e)} \tag{17}$$

where,

$$I^{(e)} = \frac{1}{2}\iiint_V \left[k_x\left(\frac{\partial T^{(e)}}{\partial x}\right)^2 + k_y\left(\frac{\partial T^{(e)}}{\partial y}\right)^2 + k_z\left(\frac{\partial T^{(e)}}{\partial z}\right)^2 - 2\left(\acute{q} - \rho c\frac{\partial T^{(e)}}{\partial t}\right)T^{(e)}\right]dV + \iint_{S_2} q_0 T^{(e)} dS_2 + \frac{1}{2}\iint_{S_3} h(T^{(e)} - T_\infty)^2 dS_3 \tag{18}$$

For the minimization of the functional *I*, use the necessary conditions

$$\frac{\partial I}{\partial T_i} = \sum_{e=1}^{E}\frac{\partial I^{(e)}}{\partial T_i} = 0, \quad i = 1,2,\dots M \tag{19}$$

where, *M* is the total number of nodal temperature unknowns.

Equations (18) and (19) can be further simplified to (20) with a note that if node *i* does not lie on S2 and S3 then the surface integrals will not appear

$$\frac{\partial I^{(e)}}{\partial \vec{T}^{(e)}} = \left[K_1^{(e)}\right]\vec{T}^{(e)} - \vec{P}^{(e)} + \left[K_2^{(e)}\right]\vec{T}^{(e)} + \left[K_3^{(e)}\right]\vec{T}^{(e)} \tag{20}$$

Step 4: Rewrite (20) in matrix form as

$$\frac{\partial I}{\partial \vec{T}} = \sum_{e=1}^{E}\frac{\partial I^{(e)}}{\partial \vec{T}^{(e)}} = \sum_{e=1}^{E}\left(\left[K_1^{(e)}\right]\vec{T}^{(e)} - \vec{P}^{(e)} + \left[K_2^{(e)}\right]\vec{T}^{(e)} + \left[K_3^{(e)}\right]\vec{T}^{(e)}\right) = \vec{0} \tag{21}$$

where, $\underset{\sim}{\vec{T}}$ is the vector of unknown nodal temperatures of the system.

$$\underset{\sim}{\vec{T}} = \begin{Bmatrix} T_1 \\ T_2 \\ . \\ . \\ . \\ T_p \end{Bmatrix}$$

Using familiar assembly process, (21) can be expressed as

$$\left[\underset{\sim}{K}_3\right]\underset{\sim}{\vec{T}} + \left[\underset{\sim}{K}\right]\underset{\sim}{\vec{T}} = \underset{\sim}{\vec{P}} \tag{22}$$

where,

$$\left[\underset{\sim}{K}_3\right] = \sum_{e=1}^{E}\left(\left[K_3^{(e)}\right]\right) \tag{23}$$

$$\left[\underset{\sim}{K}\right] = \sum_{e=1}^{E}\left(\left[K_1^{(e)}\right] + \left[K_2^{(e)}\right]\right) \tag{24}$$

$$\underset{\sim}{\vec{P}} = \sum_{e=1}^{E}\left(\vec{P}^{(e)}\right) \tag{25}$$

Step 5: Equations (22) to (25) are the equations those have to be solved after incorporating the specified boundary conditions over S_1 (11) and the initial conditions (14).

The FEA has been carried out with the use of eight node brick element approach [14,18] where each of the eight nodes has single translational degrees of freedom in the nodal x, y or z directions. For carrying these entire analysis, the initial and boundary conditions used are shown in table II. The boundary conditions are indicating the maximum temperature limits considering the combined effects of core losses and winding losses. The analysis has been carried out for design approach A shown in table III in accordance to the simulation load method of IS 11171: 1987 to have better comparision with the practical method.

Table 2. Initial & Boundary Conditons

Segment Analyzed	No. of Elements	Initial Condition	Boundary Condition
		Initial Temp. in ° C	Hot Spot Temp. of Winding in ° C
Core	240060	35	≤ 22+50*
Windings	276099	35	≤ 58+50*
Complete Assembly	-	-	≤ 70+50*

* 50 is the design ambient temperature

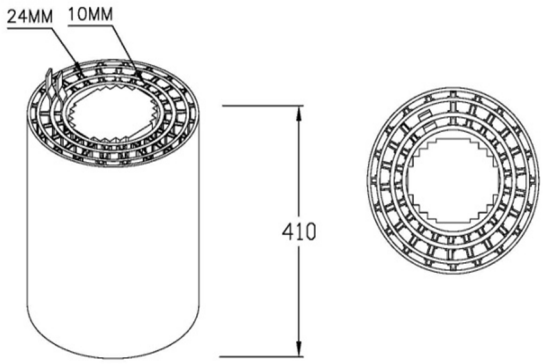

Fig 4. Coil Geometry A

Table 3. Design approach A

Flux Density	Inner Winding ID	Current Density		Spacer Size
		Secondary-Inner Winding	Primary-Outer Winding	
1.3 Tesla	210 mm	1.8 A/mm^2	2.5 A/mm^2	10 / 24 mm

The values of winding temperature are summerized in table IV for a coil geometry A as shown in Fig. 4. The values indicated are the maximum values found during the analysis at a particular node after segmentized analysis of core and winding for their specified losses respectively. The total temperature rise of the winding as a compelte assembly is calculated using (26).

$$\theta_T = \theta_C \left[1 + \left(\frac{\theta_e}{\theta_c}\right)^{1.25}\right]^{0.8} \tag{26}$$

where, θ_T is the total temperature rise of the winding, θ_e is the temperature rise of the winding due to no load losses and θ_C is the temperature rise of the winding due to copper losses.

Table 4. Temperature rise with coil geometry A

Segment Analyzed	Temperature Rise of Winding in °C					
	Primary Windings			Secondary Windings		
	U1	V1	W1	U2	V2	W2
Core	7.8	8.5	8.2	24.5	24.7	24.8
Windings	56.0	57.2	57.0	62.0	62.5	62.8
Complete Assembly	59.8	61.4	61.0	77.1	77.7	78.1

Modified Design Approach

Based on the results obtained it was decided to change the design parameters. Approach B has been adopted for further analysis. The coil geometry for the same has been shown in Fig. 5.

The values of temperature rise based on the hot spot temperatures are summarized in table VI below and the temperature distribution of complete assembly for all the three phases of primary and secondary windings have been shown in Fig. 6 and 7. The ambient temperature of 35 °C has been considered during all these calculations.

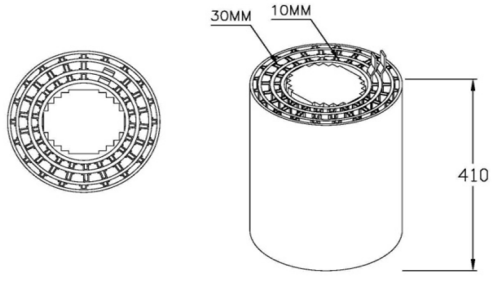

Fig 5. Coil Geometry B

Table 5. Design Approach B

Flux Density	Inner Winding ID	Current Density		Spacer Size
		Secondary-Inner Winding	Primary-Outer Winding	
1.275 Tesla	215 mm	1.8 A/mm^2	2.5 A/mm^2	10 / 30 mm

Table 6. Temperature rise with coil geometry B

Segment Analyzed	Temperature Rise of Winding in °C					
	Primary Windings			Secondary Windings		
	U1	V1	W1	U2	V2	W2
Core	7.6	8.1	7.9	23.5	23.7	23.5
Windings	54.0	54.9	54.2	49.2	49.7	49.4
Complete Assembly	57.7	58.9	58.1	64.3	64.9	64.5

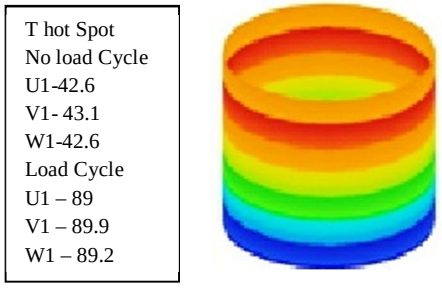

Fig 6. Temperature Distribution in Primary Winding

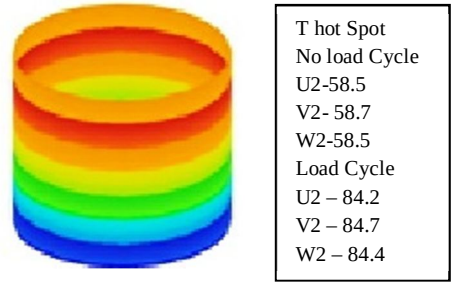

Fig 7. Temperature Distribution in Secondary Winding

In this analysis while deriving the hot spot temperatures, the effect of surrounding ambient temperature on heat dissipation as well as the effect of heat generated by the winding of one particular phase that on the other phases have not been considered.

Results

Based on the above analysis, the transformer has been subjected to heat run test at ERDA, Vadodara, Gujarat, India in accordance to the IS 11171:1987 and IS 2026:2011 by simulation load test method. The summary of the result i.e. the highest value of temperature rise obtained after heat run test has been shown in table VII.

This result indicates that with increase in duct (spacer) size, the air flow in between the winding has increased resulted into better heat transfer through convection. The obtained results are quite close to the one obtained through FEA. It also reveals that the increase in spacer size has effectively increased the resistance of the primary winding resulted into increase in active losses and ultimately the temperature rise. This has been reflected in the final results, the temperature rise of primary (outer) winding for the middle phase is 2.5 °C higher as compared to the achieved results by modified approach. However the same in middle phase of the secondary (inner) winding is differing by just 0.5 °C that too on the lower side.

Table 7. Temperature rise of transformer by simulation load method

Heat Run Cycle	Temperature Rise in °C	
	Primary Winding	Secondary Winding
	V1 Phase	V2 Phase
No Load Cycle	7.36	24.91
Load Cycle	57.9	48.11
Total Temperature Rise in °C	61.4	64.4

Conclusion

This paper reveals that the thermal behavior of dry type transformers can be estimated quite accurately with the help of 3D finite element method using Variational approach as compared to 2 dimensional approaches. This helps in adopting proper designing approach (safety factor) whereby the required level of temperature rise (thermal class) can be achieved. This consumes less time and helps in determining the safety factor without any physical development of prototype model.

The approach can further be extended to find out the thermal behavior of other electrical equipments such as generators, motors, oil cooled transformer, etc. This approach can even be modified to have higher accuracy in the results obtained either by selecting eight node break elements with each of the nodes having three translational degrees of freedom in the nodal x, y and z directions or with elements having even higher than eight nodes especially for the analysis of large power and distribution transformers or other equipments.

References

[1] H. M. Ahn, Y. H. Oh, J. K. Kim, J. S. Song and S. C. Hahn, “Experimental verification and finite element analysis of short circuit electromagnetic force for dry type transformer”, IEEE Transactions on Magnetics, vol. 48, no. 2, pp. 819-822, Feb. 2012

[2] M. R. Barzegaram, M. Mirzaie, A. S. Akmal, “Frequency response analysis in power transformer for detection of winding short circuit using quasi-static finite element and circuit based Method”, World Applied Sciences Journal 7(8), pp. 1006-1015, IDOSI Publications, 2009

[3] A. S. Reddy, M. Vijaykumar, “Hottest spot and life evaluation of power transformer design using finite element method”, Journal of Theoretical and Applied Information Technology, pp. 238-243, 2005-2008

[4] M. A. Tsili, A. G. Kladas and P. S. Georgilakis, “Computer aided analysis and design of power transformers”, Science Direct, Computers in Industry 59, pp 338-350, 2008

[5] S. C. Bell and P. S. Bodger, "Power transformer design using magnetic circuit theory and finite element analysis – A Comparison of Techniques", AUPEC 2007, Perth Western Australia, pp. 607 – 612, Dec. 2007
[6] G. B. Kumbhar and S. V. Kulkarni, "Analysis of short-circuit performance of split-winding transformer using coupled field-circuit approach", IEEE Trans. Power Del. Vol. 22, no. 2, pp. 936-943, Feb. 2007
[7] J. Hong, L Heyun, X Zihong, "Three dimensional finite element analysis of electric fields at winding ends of dry type transformer", ICEMS 2005, Proceedings of the 8th International conference on Electrical machines an Systems, Vol. 3, pp. 2136-2139, Sept. 2005
[8] L. W. Pierce, "Transformer design and application considerations for non sinusoidal load currents", IEEE IAS, 0-7803-2456-0/95, pp. 35-47, 1995
[9] A. G. Kladas, M. P. Papadopoulos and J. A. Tegopoulos, "Leakage flux and force calculation on power transformer windings under short-circuit:2-D and 3-D models based on the theory of images and the finite element method compared to measurements", IEEE Transaction on Magnetics, vol. 30, no. 5, pp. 3487-3490, Sep. 1994
[10] J. Smolka, CFD based 3-D optimization of the mutual coil configuration for the effective cooling of an electrical transformer, Applied Thermal Engineering 50, Elsevier, pp. 124-133, 2013
[11] M. Lee, H. A. Abdullah, J. C. Jofriet, D. Patel, *Temperature distribution in foil winding for ventilated dry type power transformers*, Electrical Power System Research 80, Elsevier, pp. 1065-1073, 2010
[12] M. Lee, H. A. Abdullah, J. C. Jofriet, D. Patel, *Thermal modeling of disc type winding for ventilated dry type transformers*, Electrical Power System Research 80, Elsevier, pp. 121-129, 2009
[13] Co. Wm. T McLyman, *Transformer and Inductor Design Hand book*, Marcel Dekker, Inc., New York, USA, 3rd edition, 2004, p. 10-1 -10-12
[14] Y. W. Kwon and H. Bang, The Finite Element Method using Matlab, CRC Press, 2nd edition, 2000, p. 51-70
[15] M. G. Say, *The performance and Design of Alternating Current Machines*, CBS Publishers & Distributors, Delhi, 3rd edition, 1983, p. 110, 111
[16] A. K. Sawhney, *A course in Electrical Machine Design*, Dhanpat Rai & Sons, Delhi, 1994 edition, p. 43-48
[17] S. S. Rao, *The Finite Element Method in Engineering*, Elsevier, New Delhi, 5th edition, 2011, p. 473-487
[18] S. Moaveni, *Finite Element Analysis Theory and Application with Ansys*, Pearson Education Inc., 3rd edition, 2011, p.695-697
[19] Dejan Susa, Dynamic Thermal Modeling of Power Transformers, A Doctoral Dissertation presented at Department of Electrical and Communication Engineering, Helsinki University of Technology, Espoo, Finland, August 2005
[20] Indian Standard, Specification for Dry Type Power Transformers, IS-11171, p.9-10, 1985, reaffirmed 2001